

A projection method for statics and dynamics of lattice spin systems

M. Kolesik,^{1,2} M. A. Novotny,^{1,3} and Per Arne Rikvold^{1,4}

¹*Supercomputer Computations Research Institute, Florida State University, Tallahassee, Florida 32306-4130*

²*Institute of Physics, Slovak Academy of Sciences, Dúbravská cesta 9, 84228 Bratislava, Slovak Republic*

³*Department of Electrical Engineering, 2525 Pottsdamer Street, Florida A&M University–Florida State University, Tallahassee, Florida 32310-6046*

⁴*Center for Materials Research and Technology, Department of Physics, Florida State University, Tallahassee, Florida 32306-4350*

(December 2, 2024)

A method based on Monte Carlo sampling of the probability flows projected onto the subspace of one or more slow variables is proposed for investigation of dynamic and static properties of lattice spin systems. We illustrate the method by applying it, with projection onto the order-parameter subspace, to the three-dimensional 3-state Potts model in equilibrium and to metastable decay in a three-dimensional 3-state kinetic Potts model.

The widespread use of computer simulations in many fields of physics presents a constant challenge to developing new, faster, and more efficient algorithms. This article describes a method to study dynamic and static properties of spin lattice systems. It is based on a Monte Carlo sampling of the probability flow projected onto the subspace of one or more slow variables. Here we use the order parameter. The projected information is subsequently used to reconstruct dynamic and/or static quantities. This idea was first explored by Schulman [1], and a similar approach for the dynamics of metastable decay was developed by Lee *et al.* [2] and in Ref. [3]. The present work is an extension of these developments. We show how appropriately sampled projected probability flows can be utilized to investigate static probability distributions, as well as the dynamics of lattice spin systems. The method is illustrated for three cases. The first two deal with three-dimensional, three-state Potts models in equilibrium. The ferromagnetic model at its transition temperature is considered in order to explain, for a generic situation, the basics of the method. This model is of interest also to lattice-gauge theory [4]. Next, the antiferromagnetic model below its critical temperature is included to show an unusual example of the phase structure. Although only intended as an illustration, material presented here greatly elucidates previous Monte Carlo observations of a medium-temperature phase of the model [5,6]. Our third example concerns the application to the dynamics of the metastable decay in the 3-dimensional 3-state kinetic ferromagnetic Potts model, which can be regarded as an extension of the Ising model approximation for extremely anisotropic magnetic sys-

tems [7,8]. We demonstrate the strength of the method by measuring metastable lifetimes in a region of magnetic fields in which conventional simulations are not feasible.

Consider a 3-state Potts model with the Hamiltonian $\mathcal{H} = -J \sum_{\langle i,j \rangle} \delta(\sigma_i, \sigma_j)$ where $\sigma_i \in \{0, 1, 2\}$ is the “spin” at lattice site i , and the summation runs over all nearest-neighbor pairs on a simple-cubic lattice.

Macroscopically, the system is characterized by the concentrations $\{n_0, n_1, n_2\}$, $\sum n_i = 1$, of spins in the three Potts states. These triples are mapped into an equilateral triangle representing the order-parameter space. In Figs. 1 and 2, the projection of a point onto the axis extending from the i -th corner gives the concentration n_i .

Consider a simulation using a Monte Carlo method with local updates at randomly chosen sites. At any given moment, spins can be divided into spin classes specified by the state σ of the spin and by the numbers $\{a, b, 6-a-b\}$ of its neighbors in the states $\{0, 1, 2\}$. Let $c_{ab}^\sigma(n_0, n_1, n_2)$ be the average equilibrium population of spins in the class $\{\sigma, a, b\}$, conditional on the total concentrations n_i of spins in state i . Further, denote by $p_{ab}^{\sigma\sigma'}$ the probability that a spin in the class $\{\sigma, a, b\}$ will flip to the state σ' when visited by the updating algorithm.

The central objects of the proposed method are the global flip rates $v_{\sigma\sigma'}(n_0, n_1, n_2)$:

$$v_{\sigma\sigma'}(n_0, n_1, n_2) = \sum_{ab} c_{ab}^\sigma(n_0, n_1, n_2) p_{ab}^{\sigma\sigma'}. \quad (1)$$

They contain information needed to characterize the state of the system, as well as its near-equilibrium dynamics. For example, the probability density $P(n_0, n_1, n_2)$ for the system to be found at a certain point in the order-parameter space can be calculated from the detailed-balance condition $P(n_0 + 1, n_1, n_2)v_{01}(n_0 + 1, n_1, n_2) = P(n_0, n_1 + 1, n_2)v_{10}(n_0, n_1 + 1, n_2)$ plus similar equations for the other variables.

Of special importance are the zeroes of the “drift functions” $v_{\sigma\sigma'} - v_{\sigma'\sigma}$, since they determine the extremal points of the probability densities. For the statics of the Potts model, we restrict ourselves to these zero loci.

We simulated the ferromagnetic model ($J = 1$) at its first-order phase transition temperature $T = 1.81618$ [9]. Flip-rate histograms were binned using 2^{14} equilateral

triangles covering the whole order-parameter triangle, and 10^6 configurations were typically generated. Figure 1(a) shows a schematic picture of the drift in one of the three directions. Its zero locus consists of two parts. The first one is the symmetry axis of the order-parameter triangle, and the second is an arc symmetric with respect to the axis. We only show a portion of the arc, since the statistics become insufficient far from the probability density maxima. Flows in different directions are related by rotations of $2\pi/3$. All three zero loci are superimposed in Fig. 1(b). Where three loci corresponding to different directions intersect, the probability density has a stationary point. There are three stable extrema S_i , corresponding to the three ordered phases. The three points U_i are saddle points, and the center of the triangle represents the stable, disordered phase. This example shows how one identifies candidates for stable phases from the intersections of the drift-function zero loci.

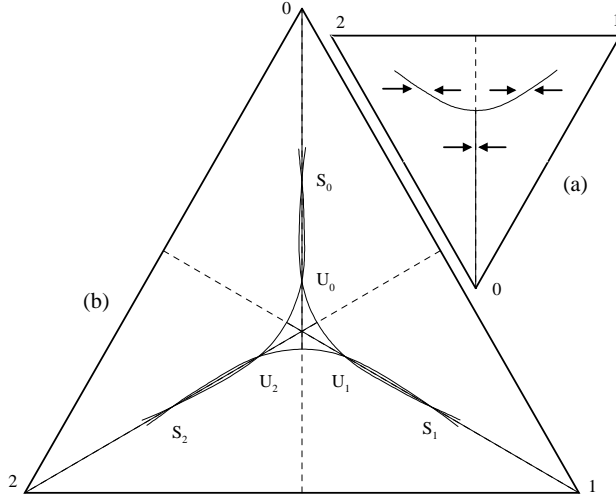


FIG. 1. (a): Zeros of the drift $v_{12} - v_{21}$ in the $1 \leftrightarrow 2$ direction for the 3-dimensional 3-state Potts ferromagnet. Light solid lines are stable loci, while dashed lines are unstable. Heavy arrows indicate the direction of the probability flow. (b): Zero loci for the three directions superimposed. The center of the triangle and the points labeled S_i are stable. The probability density P has local maxima there. The points U_i are saddle points. Data were taken during simulation on a lattice of size 20^3 at the first-order transition temperature.

Next, we turn to the antiferromagnetic Potts model ($J=-1$). Because of the sublattice-symmetry breaking, we sampled the flip rates for each sublattice separately.

Figure 2 shows the union of the zero loci of the drift functions in all three directions. As in the ferromagnetic case, for each direction there is the symmetry induced straight line (triangle axis) and a nontrivial part, which is here a closed curve. A closer inspection reveals that the closed-curve parts of the zero loci have several interesting properties:

1. The closed loci for the three different directions are *identical* and can be accurately parameterized by

$$\{m \cos t + r \cos 2t, m \sin t - r \sin 2t\}, t \in \langle 0, 2\pi \rangle. \quad (2)$$

2. Positions of the sublattices on this curve are correlated in such a way that their distance (sublattice magnetization difference $|AB| = 2m$ in Fig. 2) is constant.

3. There are finite-size effects in the diameter and shape of the curve, but there is no sign that it separates into three distinct components.

We stress that the only observed deviations from these properties are numerical uncertainties on the order of the discreteness of the order-parameter space. On lattices smaller than 32^3 , we sampled complete flip-rate histograms as in the ferromagnetic case. On larger lattices, we only measured flip rates at isolated points of the order-parameter space (generating typically 5×10^4 configurations). The data were then interpolated and used for finding the roots of the drift functions. In this way, we were able to confirm the above observations even with lattices as large as 64^3 by measuring flip rates only in the vicinity of the expected zero locus. In fact, having located two points we can predict the rest with an accuracy suggesting that the parameterization (2) may be exact.

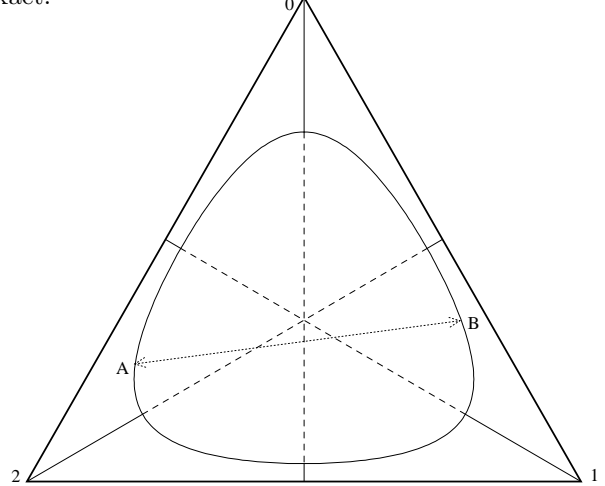


FIG. 2. Zero locus of the drift functions $v_{\sigma\sigma'} - v_{\sigma'\sigma}$ of the 3-dimensional 3-state Potts antiferromagnet at $T = 1.0J$. The dashed sections of the triangle axes are unstable in directions perpendicular to the axes. The solid parts are stable. The closed, solid curve is stable in all three directions. This curve, obtained for a 64^3 lattice, represents the degenerate maximum of the probability density of a sublattice location in the order-parameter space.

The above observations mean that the probability density has a degenerate maximum. Whereas the magnitude of the sublattice magnetization difference is fixed, it can point in an arbitrary direction. Thus, a system with only three microscopic states exhibits a continuous symmetry on the macroscopic scale. This is the rotationally symmetric phase which was found in recent Monte Carlo simulations [5,6]. However, the conventional probability density sampling technique did not provide completely con-

vincing evidence that this symmetry is not (weakly) broken. The present approach, however, gives much stronger support for the symmetric phase. It locates the extrema of the probability density without sampling the distribution itself. With relatively modest statistics, the symmetric property was corroborated with an accuracy approaching the limit imposed by the discreteness of the order-parameter space. Such precision would require an enormous statistical effort if one were to investigate the sampled distribution directly.

We intend to address open problems concerning the low-temperature phase of the antiferromagnetic Potts model in future work. The method presented here provides a useful tool for such an undertaking.

Our final example deals with the metastable decay in the ferromagnetic Potts model with the Hamiltonian $\mathcal{H} = -J \sum_{\langle i,j \rangle} \delta(\sigma_i, \sigma_j) + H \sum_i [\delta(0, \sigma_j) - \delta(1, \sigma_j)]$. Here, we have added a term describing the interaction with the external field H . With this choice of the external field, the model can be regarded as an extension of the kinetic Ising model, which can serve as an approximation for nanoscale ferromagnets [7,8]. The third spin state of the present model can mimic local magnetization “perpendicular” to the external field and allows for “finite anisotropy.” The Glauber dynamics with updates at randomly chosen sites is used throughout the rest of the paper. Time is measured in Monte Carlo Steps per Spin (MCSS).

An essential quantity related to the metastability is the lifetime τ , defined as follows. All spins are initialized in state 0, the temperature T is fixed well below its critical value T_c , and an external magnetic field H favoring state 1 and disfavoring state 0 is applied. The field does not interact with spins in state 2. This initial state is metastable and decays through the nucleation and subsequent growth of stable-phase droplets. The average time needed to reach a configuration with half of the system in the stable phase is the lifetime. The difficulty is that realistic models, subjected to “experimentally reasonable” magnetic fields, have lifetimes which are extremely long in terms of the Monte Carlo time. Here we describe a significant extension of the method proposed in Refs. [1–3]. This allows us to obtain lifetimes in arbitrarily weak fields without prohibitively lengthy simulations.

The projected flip rates are defined, as in the static case, in terms of the spin-class populations $c_{ab}^\sigma(n)$ and flipping probabilities $p_{ab}^{\sigma\sigma'}$:

$$g(n) = \sum_{ab, \sigma} c_{ab}^\sigma(n) p_{ab}^{\sigma 1}, \quad s(n) = \sum_{ab, \sigma} c_{ab}^\sigma(n) p_{ab}^{1\sigma}. \quad (3)$$

Here, we parameterize g and s only by the total number n of spins in state 1. Thus, all the population data are projected from the order-parameter space onto a one-dimensional histogram. The rates g and s correspond to growth and shrinkage of the stable phase. They depend

on the external field and on the way the configurations are generated, as explained below.

The flip rates are used to map the metastable-decay dynamics onto a one-dimensional absorbing Markov chain. We assign to all configurations with n overturned spins a single state n in the chain. The one-dimensional dynamics is given by the flip rates. From state n we have the probability $g(n)$ of jumping to state $n+1$, the probability $s(n)$ of jumping to $n-1$, and the probability $1-s(n)-g(n)$ of remaining in the current state. This random walk starts at $n=0$ and terminates when it reaches $n=N$, corresponding to a stopping criterion which we chose to be $N = V/2$, with V the volume of the system. Using standard methods from the theory of absorbing Markov chains [2,10], we obtain the mean lifetime τ and the total average time $h(n)$ (with $h(N) = 0$, measured in MCSS) spent by the random walker in the state n in terms of the flip rates as follows:

$$\tau = \sum_{n=0}^{N-1} h(n), \quad h(n-1) = \frac{V^{-1} + s(n)h(n)}{g(n-1)}. \quad (4)$$

How accurately these formulas reproduce the lifetime depends on exactly how the class populations are sampled. One option is to measure class populations in zero external field in an equilibrium ensemble with conserved order parameter for each needed value of n [1,2]. Such data can be used to estimate the lifetime in very weak fields, but one observes that in strong fields the lifetime is underestimated because the class populations in the vicinity of the top of the free-energy barrier are not reproduced well by the equilibrium ensemble.

The simple but important improvement presented here is the way the class populations are measured. At any time, the system is only allowed to have n , the number of spins in the stable phase, larger than a time-dependent lower bound, n_{\min} . Simulation starts with $n_{\min}(t=0) = 0$, and n_{\min} is increased slowly. The class populations c_{ab}^σ are sampled during this forced-escape simulation with an applied external field and are subsequently used to calculate the lifetime from Eqs. (3,4). Why does this work? If the rate of increase of n_{\min} is sufficiently small, the system always produces the “correct” configurations as if there were no forcing. While deep in the metastable free-energy well, forcing prevents the system to return to $n < n_{\min}$, but it still allows it to thermalize and generate metastable configurations with n at and slightly above n_{\min} . As n_{\min} increases, the procedure scans the configurations along the escape path from metastability. When n_{\min} approaches the top of the free-energy barrier, the system has a better chance to escape, and the stable phase grows too quickly to equilibrate. There is nothing to prevent escape, because there is no upper bound on n which would otherwise cause unwanted thermalization. Thus, the system is free to escape through a natural nonequilibrium sequence of configura-

tions.

The speed dn_{\min}/dt of the moving lower bound is the crucial parameter. In the limit $dn_{\min}/dt \rightarrow 0$, the escape is completely free. To approach this limit in practice, one performs a series of measurements and determines a value of dn_{\min}/dt below which the estimated lifetime is insensitive to the choice of dn_{\min}/dt . Another computationally important aspect is to obtain sufficient statistics for the forced escapes, since the class-population data tend to be noisy at and beyond the top of the free-energy barrier. We measured about 10^3 escapes at rates up to $dn_{\min}/dt \approx 10^{-3}$ MCSS $^{-1}$ for the simulations presented here.

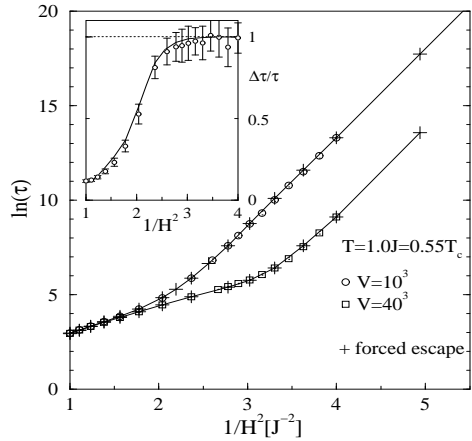


FIG. 3. The metastable lifetime of a 3-dimensional 3-state kinetic Potts ferromagnet as a function of the magnetic field for two system sizes. Symbols are simulation results (with error bars smaller than the symbol size), and lines connect the points (+) calculated from the class-population data sampled by the forced-escape method. The inset shows a comparison of the measured (circles) and calculated (line) relative standard deviation of the lifetime.

Figure 3 shows a comparison between the lifetimes obtained from direct simulations and those calculated with the forced-escape method. The agreement is excellent for lifetimes in the whole region accessible to direct simulations. Moreover, the forced escape method can provide lifetime estimates deep in the region of weak fields, where direct simulation is practically impossible. We emphasize that having measured the class populations, one can utilize them to calculate lifetimes for an arbitrary local dynamic with random updates. We can e.g. calculate what the lifetimes would be if we used the Metropolis instead of the Glauber dynamic simply by replacing the flip probabilities $p_{ab}^{\sigma\sigma'}$. This is based on the observation that although different dynamics produce different flip rates, the class-populations remain close to local equilibrium and are therefore similar for all dynamics that obey detailed balance.

In a similar way as the lifetime τ , one can use the flip rates to calculate higher moments of the lifetime probability distribution [2]. The inset in Fig. 3 shows the

relative standard deviation $\Delta\tau/\tau$ as a function of the field. The agreement between the directly simulated results and those based on the forced-escape method (solid line) is good. For a quantitative description of the form of τ and $\Delta\tau/\tau$, see Refs. [7] and [8].

In summary, we propose a new method to study the dynamic and static properties of lattice spin systems. It consists in Monte Carlo sampling of the spin-class populations in a projected subspace. These are subsequently used to calculate the spin-flip rates. In the static case, the knowledge of the flip rates is equivalent to the information contained in the probability density. However, the accuracy of the method is much better than with direct distribution sampling. We have demonstrated this on the example of the 3-state antiferromagnetic Potts model.

The flip rates can be also utilized to obtain dynamic characteristics of the systems, such as lifetimes, in very weak fields where ordinary simulations are not feasible. Although the resulting dynamic is only an approximation, it provides accurate estimates. The detailed information about the class populations enables one to calculate the lifetime for an arbitrary dynamic with updates at randomly chosen sites, independently of the dynamic used during the data sampling.

We appreciate helpful discussions with S. W. Sides. This research was supported by NSF Grants No. DMR-9520325 and DMR-9634873, FSU-MARTECH and FSU-SCRI (DOE Contract No. DE-FC05-85ER25000).

- [1] L. S. Schulman, J. Phys. A: Math. Gen. **13**, 237 (1980).
- [2] J. Lee, M. A. Novotny and P. A. Rikvold, Phys. Rev. E **52**, 356 (1995).
- [3] M. Kolesik, M. A. Novotny, P. A. Rikvold and D. M. Townsley, in *Computer Simulation Studies in Condensed-Matter Physics X*, edited by D. P. Landau, K. K. Mon and H.-B. Schüttler (Springer, Berlin), in press.
- [4] B. Svetitsky and L. Yaffe, Nucl. Phys. B **210**, 423 (1982).
- [5] M. Kolesik and M. Suzuki, J. Phys. A: Math. Gen. **28**, 6543 (1995).
- [6] R. K. Heilmann, J. S. Wang and R. H. Swendsen, Phys. Rev. B **53**, 2210 (1996).
- [7] P. A. Rikvold, H. Tomita, S. Miyashita and S. W. Sides, Phys. Rev. E **49**, 5080 (1994); P. A. Rikvold and B. M. Gorman, in *Ann. Rev. Comp. Phys. I*, edited by D. Stauffer (World Scientific, Singapore, 1994), p. 149.
- [8] H. L. Richards *et al.*, J. Magn. Magn. Mater. **150**, 37 (1995); J. Appl. Phys. **79**, 5749 (1996); Phys. Rev. B **54**, 4113 (1996); **55**, 11521 (1997).
- [9] W. G. Wilson and C. A. Vause, Phys. Rev. B **36**, 587 (1986).
- [10] M. A. Novotny, Phys. Rev. Lett. **74**, 1 (1995); **75**, 1424(E) (1995); Comput. in Phys. **9**, 46 (1995).